Lipid Domains

DOI: 10.1002/anie.201004470

Crystalline Lipid Domains: Characterization by X-Ray Diffraction and their Relation to Biology

*Roy Ziblat, Leslie Leiserowitz, and Lia Addadi**

lipid domains · lipids · membranes · X-ray diffraction

***B**iological membranes comprise thousands of different lipids, differing in their alkyl chains, headgroups, and degree of saturation. It is estimated that 5 % of the genes in the human genome are responsible for regulating the lipid composition of cell membranes. Conceivably, the functional explanation for this diversity is found, at least in part, in the propensity of lipids to segregate into distinct domains, which are important for cell function. X-ray diffraction has been used increasingly to characterize the packing and phase behavior of lipids in membranes. Crystalline domains have been studied in synthetic membranes using wide- and small-angle X-ray scattering, and grazing incidence X-ray diffraction. Herein we summarize recent results obtained using the various X-ray methods, discuss the correlation between crystalline domains and liquid ordered domains studied with other techniques, and the relevance of crystalline domains to functional lipid domains in biological membranes.*

1. Cell Membrane Lipids and X-Ray Scattering

Cell membranes are thin sheets composed of two opposing lipid monolayers. They delimit cells and cell compartments, and function as selectively permeable barriers, regulating molecular trafficking to their functional sites. In addition to their function as boundaries, membranes also act as active interfaces at which biological processes occur. Cells in fact control the reaction rates of specific biological processes by altering the lipid composition of their membranes. Chemical reactions occur in some cases faster at the two-dimensional (2D) interface than in 3D bulk media, owing to the confined rotational and translational diffusion. Cell plasma membranes usually comprise only 2–5 % of the entire membrane weight, whereas the major part resides within the cell, in its organelles.[1] The ratio of membrane surface area per cell volume is therefore exceptionally high, indicating that processes occurring at interfaces are essential for cell survival and function.

Lipids in the bilayer segregate into different lipid domains. Ordered lipid domains, also referred to as "lipid rafts", have been studied intensively ever since their importance was established as organizing centers for the assembly of signaling molecules and in membrane protein trafficking.[2] Membrane proteins selectively partition in these domains, which differ in lipid composition and organization. It follows that lipid organization into domains is directly or indirectly related to the control of cell function. Whether and to what extent these domains have an ordered periodic arrangement that can be detected by X-ray diffraction is still a debated issue, and is discussed in this Minireview.

1.1. Lipid Molecules

Cell membrane lipids can be sorted into three main groups: the glycerolipids, fatty acid esters of glycerol, the sphingolipids, fatty acid amides of the aliphatic amino alcohol sphingosine, and sterols (Scheme 1). The most abundant sterol in mammalian cells is cholesterol. Cholesterol plays an important role in determining the dynamic and mechanical

[*] R. Ziblat, Prof. L. Addadi
Department of Structural Biology, Weizmann Institute of Science
76100 Rehovot (Israel)
Fax: (+972) 8-934-4136
E-mail: lia.addadi@weizmann.ac.il
Homepage: http://www.weizmann.ac.il/sb/faculty_pages/Addadi/home.html
Prof. L. Leiserowitz
Department of Materials and Interfaces
Weizmann Institute of Science
76100 Rehovot (Israel)

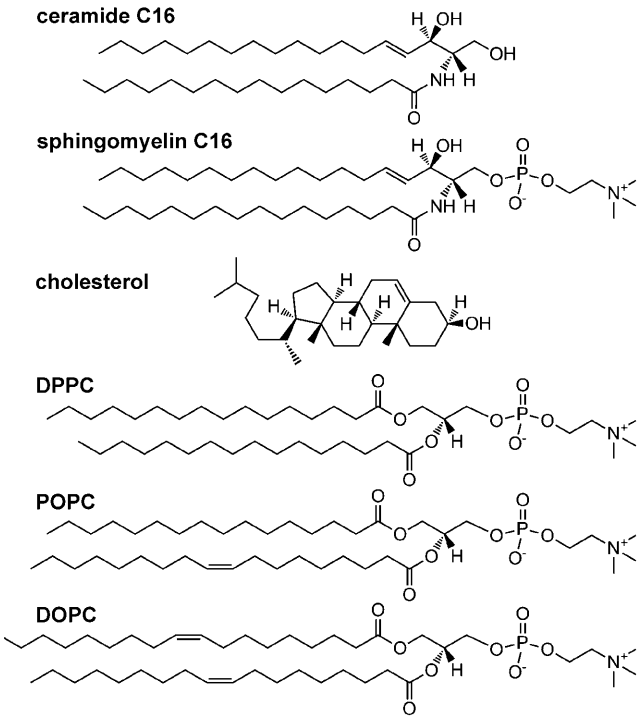

Scheme 1. Structural formulas of representative sphingolipids, cholesterol, and glycerolipids.

properties of membranes. When accumulated by cells in excess, cholesterol participates in several pathologies[3] such as atherosclerosis[4] and cataract.[5] Large amounts of cholesterol monohydrate crystals are found in gallstones[6] and in foam cells[7] at the site of atherosclerotic plaques.

Phosphocholine derivatives of both glycerolipids and sphingolipids comprise the group of lipids having the highest concentrations in cells.[8] Unsaturated lipids such as palmitoyl-oleoyl-phosphatidyl-choline (POPC) and di-oleoyl-phosphatidyl-choline (DOPC), which have one or more *cis* double bonds in the fatty acid chains, cannot pack in ordered bilayer structures because the double bonds create kinks in the alkyl chains. Not only are these molecules unable to form crystalline domains in vitro, but they are known to concentrate in the disordered regions of the cell membrane.[8]

In contrast, saturated lipids such as di-palmitoyl-phosphatidyl-choline (DPPC) and sphingomyelin (SM) and its precursor ceramide are capable of packing in ordered arrays in artificial lipid layers because of the linear geometry of the alkyl chains. Primarily DPPC,[9] and SM[10] and ceramide[11] were thus studied by X-ray diffraction, as representatives of saturated glycerolipids and sphingolipids, respectively. The so-called detergent-resistant membrane domains (DRMs), directly extracted from cell membranes, were found to contain elevated amounts of cholesterol and sphingomyelin, which were hence considered to be the main players in lipid rafts.[2b,12]

Roy Ziblat obtained a BSc degree in Physics and Mathematics in 2003 and an MSc degree in Physics in 2005, both at the Hebrew University of Jerusalem, for work on photonic crystals and the implementation of surface plasmons on cells. He obtained a PhD degree from the Weizmann Institute of Science, Rehovot (Israel) in the Structural Biology Department, characterizing lipid domains by X-ray diffraction. He is currently a postdoctoral fellow studying lipid membranes.

Lia Addadi obtained her BSc and MSc degrees in Organic Chemistry, and a PhD in Structural Chemistry from the Weizmann Institute of Science in 1979. She was appointed Associate Professor at the Weizmann Institute in 1988 and Full Professor in the Department of Structural Biology in 1993. Her research interests center on stereochemistry and molecular recognition at biological interfaces, biomineralization in organisms, mechanisms of cell adhesion, and the structure and antibody recognition of organized molecular assemblies, in particular of lipid domains in cell membranes.

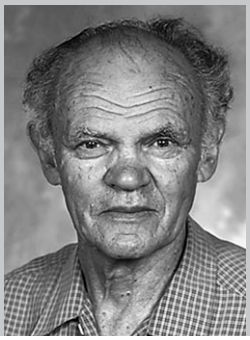

Leslie Leiserowitz studied Engineering and Physics in Cape Town (South Africa) and solid-state chemistry at the Weizmann Institute of Science. After completing postdoctoral studies in Heidelberg (Germany) he returned to the Weizmann Institute, where he collaborated with M. Lahav on reaction pathways in crystals. His more recent work has focused on pathological crystallization (cholesterol, formation of biogenic hemozoin) and laser-induced alignment of crystal films.

1.2. X-Ray Studies

The first X-ray studies on lipids were performed in the 1920s on 3D crystals of dried lipids, providing insight on interactions of the hydrocarbon chains. The structural information provided by these first studies was questioned, however, because the lipids were not always organized in a lamellar structure and the crystals contained impurities.[13] Starting in the late 1970s, however, studies on hydrated lipid sheets were performed by X-ray scattering, providing the first knowledge on the spacing and thickness of the lamellar structures.[14] Identification of variations in these parameters indicated phase transitions or separation. With the development of grazing incidence X-ray diffraction (GIXD) at liquid interfaces in the late 1980s[15] a real breakthrough in the area was achieved, enabling measurements of single lipid sheets at the air–water interface. Probably the most important conceptual contribution of these early studies was the proof that monolayer films of amphiphilic molecules can spontaneously self-assemble in 2D crystalline domains,[16] albeit small and highly dynamic, as had been suggested by prior studies.[17] The conventional notion, based mainly on pressure–area isotherm data, was that such layers cannot be crystalline unless

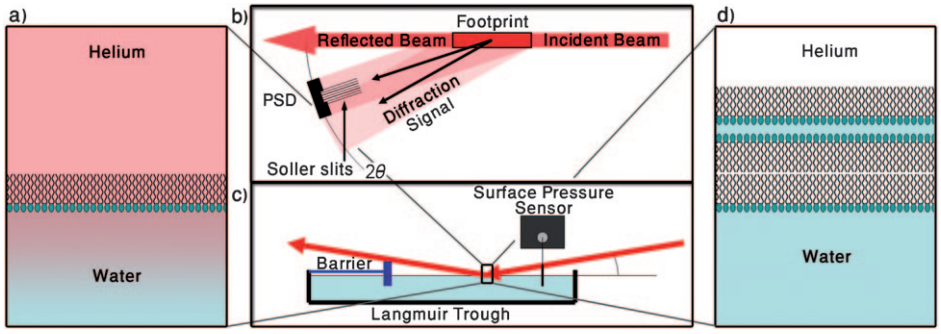

Figure 1. Scheme of GIXD performed on a monolayer (a) and collapsed layers (d). The thin layers are deposited on a Langmuir trough at the air–water interface (b, c) and diffraction signals are collected by a position-sensitive detector (PSD), which scans the sample along the angle θ; the signals lack periodicity along the vertical axis. Reflectivity measurements provide an averaged electron density profile of the sample, from which reliable and detailed information regarding thickness and undulation of the sample can be derived. Surface and bulk properties such as surface pressure of the lipid sheet, temperature, pH, salt concentration, and inclusion of protein or other molecules can be controlled. When the monolayer is compressed beyond a certain surface pressure, the monolayer may, depending on the sample composition, collapse into multilayers. Measurements performed on collapsed multilayers lack information on the number of layers, homogeneity, surface pressure, and the water spacing between the layers. In addition, the air–water interface constrains the sheet to be flat and this may lead to distortions in lipid packing.

compressed. The diffraction studies on lipid monolayers proved otherwise.

1.3. X-Ray Methods

The main methods used for studying crystalline lipid domains in thin layers are presently small- and wide-angle X-ray scattering (SAXS and WAXS), and GIXD, which may be performed on monolayers, bilayers, or multilayers under different conditions.

Conventional X-ray scattering experiments result in diffracting intensities proportional to the scattering sample volume. When this method is used on 2D films the low volume leads to undetectable X-ray signals. In GIXD, the X-ray beam strikes the sample at an incident angle at which evanescent waves, which have an exponentially decaying electromagnetic field (colored red in Figure 1a), occur, and the supporting bulk does not contribute to background scattering. Therefore, the measurement is most sensitive to samples at the interface, such as monolayers or collapsed multilayers (Figure 1). Monolayers, however, are not ideal models of cell membranes, because the hydrophobic part of the molecules is exposed to the atmosphere. Thus the interaction with an opposing lipid leaflet, which is the case in bilayer membranes, is lacking. Hydrated bilayers are preferable in this respect.

To guarantee preservation of the structural integrity of a membrane bilayer with hydrophobic interior and hydrophilic external surfaces, wetting on both sides of the bilayer is required. However, because of the strong X-ray background scattering contribution of liquid water, GIXD experiments on lipid bilayers are very difficult to perform. One technique for performing GIXD on single lipid bilayers is based on the use of high-energy X-ray beams, where beam attenuation from the water is decreased (Figure 2a).[9e,18] A new methodology, which has proven successful for samples supported on a polymer cushion, involves irradiating the sample with lower energy X-rays and maintaining a thin (<1 μm) water layer on top of the bilayer sample (Figure 2b).[9g,19] This GIXD technique at high humidity provides a relatively strong signal, enabling studies on crystalline domains with low diffraction intensity (Figure 3).

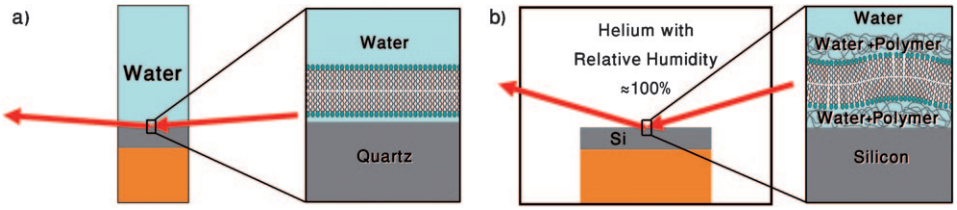

Figure 2. a) Scheme of GIXD performed on single bilayers using a high-energy beam of 18–23 keV ($\lambda = 0.54$–0.7 Å).[9e,18] Lipid bilayers have until now been deposited directly on the supporting silicon wafers: a 10 Å thick water layer is entrapped between the wafer and the bilayer. The diffusion rate of the lipids within the bilayer is substantially decreased by the interactions with the wafer which interfer with the fluid nature of the membrane;[49] the bilayer is flat and proteins embedded in the membrane cannot diffuse freely.[50] These drawbacks may be partially compensated by depositing the lipid samples on the supporting wafers on top of a highly hydrated polymer cushion. b) The samples are measured in a humidity chamber at close to the dew point and are supported on the polymer cushion. The sample is irradiated with X-rays of 9.5 keV ($\lambda = 1.3$ Å) and a thin (<1 μm) water layer is maintained on top of the bilayer sample.[9g,19] Reflectivity measurements are difficult to perform in this setup, concentrations of salts or pH cannot be adjusted, and only pure water can be used. Proteins and other molecules believed to be embedded in membranes can in principle be introduced.

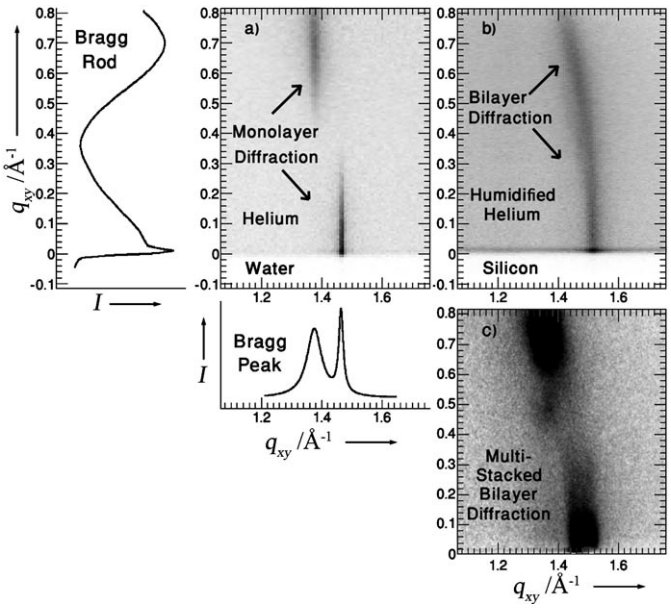

Figure 3. X-ray diffraction images obtained from: a) GIXD of a DPPC monolayer deposited at the air–water interface at 7 °C; b) GIXD of a DPPC bilayer sandwiched by a polymer cushion and deposited on a silicon wafer at 7 °C; c) WAXS of multistacked bilayers of DPPC/DOPC (9:1) deposited on a Si wafer and performed at a grazing incident angle and ambient temperature.[9b] The smearing of the peaks in (b) is due to a 10° undulation of the bilayer. The strong intensity obtained by WAXS can lead to satellite effects, seen in (c) next to the main peak.[51] X-ray data analysis: The data are represented by the scattering vector q, which is directly related to the diffraction angle, measured in reciprocal units [Å^{-1}]. Integration of (a) along q_{xy} provides a Bragg rod plot, exemplified to the left of (a). Similarly, integration along q_z provides Bragg peak plot, exemplified below (a). The q_{xy} positions of the Bragg peaks yield the lattice repeat distances $d = 2\pi/q_{xy}$, which may be indexed by the two Miller indices h,k to yield the unit cell. The full width at half-maximum (FWHM) of the Bragg peaks yields the lateral 2D crystalline coherence length $L_{xy} \approx 0.9(2\pi)/\text{FWHM}\ (q_{xy})$. The Bragg rod profile along q_z similarly gives a measure of the thickness of the crystalline film.[16]

Small-angle X-ray scattering (SAXS, Figure 4) is a method used to determine average sizes of particles in solution. SAXS was proven to be a useful tool for studying lamellar structures, providing information on lipid bilayer phases, spacings, and thicknesses in the range of a few nanometers and up to tens of nanometers.[20] Wide-angle X-ray scattering (WAXS) provides information on lipid packing at the Å scale when crystalline phases exist in the bilayers. Information on the molecular tilt can be obtained by using oriented samples of multilayers. SAXS/WAXS studies performed on multilamellar vesicles provide additional information on the correlations between the lipids by providing an order parameter within the lipid sheets.

2. Structural Parameters of Crystalline Lipid Domains

X-ray diffraction signals from lipid layers are primarily obtained from the hydrophobic part of the molecules, implying that the hydrophilic part is not well ordered or that its contribution to the signal is weak relative to that of the chain, because the constituent atoms do not scatter in phase. The "crystalline domains" may be described as small, highly dynamic monolayer or bilayer arrays of lipids, ordered such that their organization in a periodical lattice results in discrete constructive interference of the X-ray reflected beams. The diffraction of lipid domains is usually characterized by few 2D peaks for mixed phases packing in the so-called liquid ordered (l_o) phase. Despite these drawbacks, a surprising wealth of information can be derived from this apparent dearth of data, specifically from the peak position, shape, and width (derived from analysis of Bragg peaks and Bragg rods, Figure 3).

2.1. Unit Cell Packing and Crystallinity

Saturated glycerolipids and sphingolipids: Monolayers and bilayers composed purely of saturated alkyl chains display similar characteristics in unit cell dimensions, which vary little for different lipids, and have similar projected unit cell dimensions ranging between 5.0×7.5 Å^2 and 4.5×8.7 Å^2, if the molecules are not tilted (Figure 5).[21,9g] The domain sizes range between a few nanometers to tens of nanometers. Although these differences may appear subtle, they are also highly reproducible and specific.

Ceramide (Cer) spontaneously forms crystalline monolayer domains[11c,22] with an average diameter of roughly 15 nm, when spread at the air–water interface (Figure 5). In contrast to ceramide, sphingomyelin, which has the ceramide backbone, does not form crystalline domains unless it is

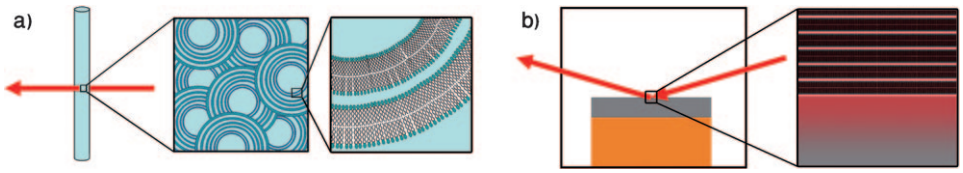

Figure 4. a) SAXS and WAXS of multilamellar vesicles (MLVs) and b) multistacked lipid bilayers. The sample preparation for the SAXS/WAXS studies is usually straightforward. In the lipid studies the X-ray beam transverses a thin-wall capillary filled with hydrated lipid samples in the form of multilamellar vesicles (a), or multilayer stacks supported on silicon wafers, where more than a thousand lipid bilayers are deposited (b).[52] The signal-to-noise ratio of the diffracted signal is by far the highest in the WAXS method, relative to GIXD. It is possible that each of the bilayer films within a sample has different characteristics and the diffraction signal is an average of all. It is also unclear how much juxtaposed bilayer films interact. The supported samples are measured at an incident angle below critical, similar to GIXD. However, owing to the beam thickness, the spot size spreads over at least 20 mm. Without the use of a beam collimator, angular resolution is reduced, especially at wide angles.

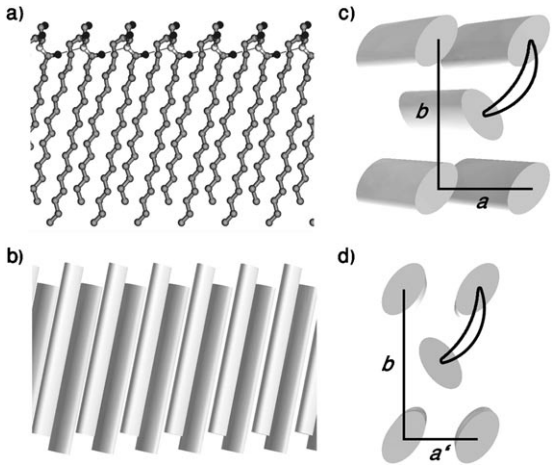

Figure 5. a) Schematic representation of a ceramide monolayer. b) Alkyl chains are represented by rods. c) Top view of (b) shows the repeating unit cell of the crystalline domain with dimensions a,b and a γ angle $\approx 90°$. Chains are linked in pairs, as shown arbitrarily for one pair. d) Projected unit cell viewed along the rod axis, with dimensions a',b ($a' < a$).

subjected to high compression.[10a,d,23] Sphingomyelin's lack of crystallinity was attributed to its large hydrophilic headgroup (Scheme 1), which disturbs the molecular packing of the thin hydrophobic moiety, leading to the so-called "umbrella effect".[24] The hydrophilic headgroup does not participate in the crystalline packing, but plays a role in determining the structure. A corollary of the umbrella effect is that molecules with small headgroups such as cholesterol and ceramide readily form mixed phases with SM, because they dilute the interactions between the SM bulky headgroups. Unlike SM, DPPC does, however, spontaneously form crystalline domains at the air–water interface at negligible surface pressure, even though it shares the same phosphocholine headgroup.[9c,d,g] In addition, DPPC, SM, and ceramide form mixed domains with cholesterol, all of which show the same structural behavior.[9g,10e,19] Such mixtures of cholesterol and saturated lipids form, even at negligible surface pressures, ordered lipid domains with molecular spacings depending on the cholesterol/lipid ratios.[9f,10d]

Cholesterol: As a monolayer at the air–water interface cholesterol spontaneously forms crystalline domains with trigonal supercell dimensions $a = b = 11.4$ Å, $\gamma = 120°$ and diameter of approximately 10 nm. The cholesterol molecule is aligned normal to the water yielding an area per molecule of 38 Å^2,[25] and its exocyclic chains are disordered. In the bilayer, the molecules are tilted by 19°, with their exocyclic chains partially interdigitated, leading to a well-packed structure with a relatively high coherence length of 40–60 nm and a rectangular unit cell of 10×7.5 Å^2.[9g,18b,25,26] This unit cell structure corresponds to the bilayer of the macroscopically metastable monoclinic phase of Chol.H_2O. Once the bilayers stack to form multilayers, with ordered water molecules interleaved between the bilayers, the structure spontaneously transforms into the triclinic monohydrate phase, which incorporates the 12.4×12.4 Å^2 ($\gamma = 100.8°$) bilayer motif.[27]

2.2. Size of the Crystalline Domain

The crystalline domain typically contains between a few tens to a few thousands of molecules. These limited sizes are in good agreement with those measured for "lipid rafts" in cell membranes,[28] but are in contrast to the physical notion dictating that 2D crystals may not be formed spontaneously, as inferred from theoretical physics.[29] One explanation of this apparent contradiction is that the roughly 5 nm thick lipid bilayer has a third dimension stabilized by multiple interactions between alkyl chains. The crystalline arrays cannot, however, grow to larger sizes primarily because of the large thermal motion and diffusion rate of the molecules. Furthermore, X-ray diffraction techniques detect only periodical structures. It is conceivable that the crystalline domains are surrounded by a less ordered population of lipid molecules. This boundary population would effectively lower the line tension between adjacent domains or with the surrounding disordered lipid environment.

Relevant to this issue is a suggestion concerning the behavior of mixtures of saturated lipids with lipids having two unsaturated alkyl chains, for example, mixtures of DPPC and DOPC.[30] Such systems are expected to phase separate into ordered and disordered domains, the size of which is expected to increase as equilibrium is approached, in order to reduce the line tension at the domain boundaries. Brewster et al. suggested that the addition of a "hybrid lipid" with one saturated and one nonsaturated alkyl chain, for example, POPC, might serve to lower the line tension, thus driving the system to form smaller domains.[30,31] In agreement with this prediction, GIXD measurements performed on monolayers composed of DPPC/DOPC/POPC with DPPC/DOPC = 1:1 showed a dramatic but anisotropic decrease of the coherence length from 115 to 30 Å when the proportion of POPC in the mixture is increased.[53]

2.3. Structural Comparisons between Monolayers, Bilayers, and Multilayers

Typically the structural differences determined from X-ray diffraction measurements performed on samples of lipid monolayers, bilayers, or multilayers are not substantial. We chose to show here, however, cases where significant dissimilarities are found, in order to illustrate their possible significance in terms of the molecular interactions that generate them.

Figure 6 shows the d-spacing of monolayers and bilayers composed of SM/Chol,[10d,19] DPPC/Chol,[9f,g] and Cer/Chol[22] (Cer/Chol bilayer data are taken from Ref. [53]). The pure cholesterol monolayer has one diffraction peak at $q_{xy} = 1.09$ Å^{-1}. At increasing concentrations of SM, DPPC, or Cer, the monolayer shows one mixed crystalline phase designated by one broad Bragg peak. The peak position is constant at low cholesterol concentrations and shifts linearly to higher q_{xy} at higher lipid concentrations. The lipid molecules are perpendicular to the layer plane even at negligible surface pressure.

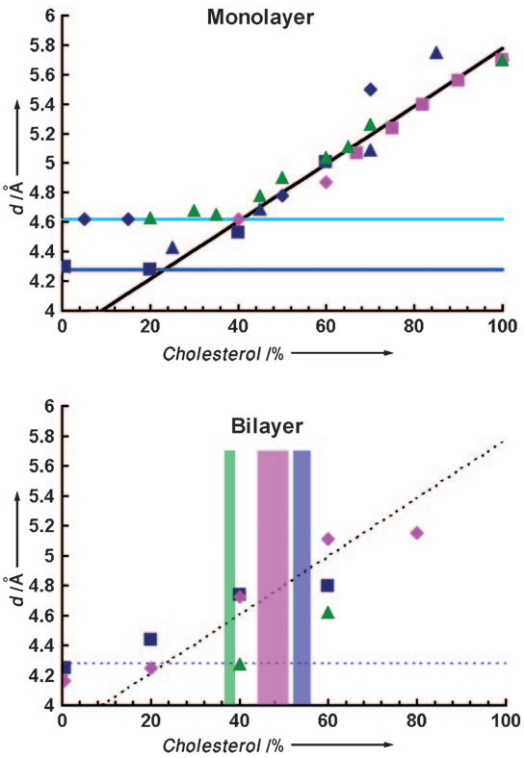

Figure 6. *d*-Spacing in monolayers (top) and bilayers (bottom) of mixed phases as a function of cholesterol concentration: SM/Chol (green), DPPC/Chol (blue), and Cer/Chol (magenta). Dark blue line: data measured at 7 °C; light blue line: data measured at 25–30 °C. Monolayer data was recorded at 20 mN m^{-1}, 23 °C (violet ◆ and ▲),[9f] at 30 mN m^{-1}, 7 °C (violet ■),[9g] at 30 mN m^{-1}, 7 °C (magenta ◆), at ≈0 mN m^{-1}, 7 °C (magenta ■),[22] and at 25 mN m^{-1}, 30 °C (green ▲).[10d] Bilayer data was recorded at 30 mN m^{-1}, 7 °C.[9g,19] Colored stripes represent the estimated cholesterol nucleation threshold for mixtures with SM (green), Cer (magenta), and DPPC (violet).

The position of the plateau at low cholesterol values appears to depend on temperature. In contrast, the slope of the linear dependence of the *d*-spacing at high cholesterol concentrations is independent of temperature (7–30 °C) and surface pressure (0–30 mN m^{-1}). The slope is identical for SM/Chol, DPPC/Chol, and Cer/Chol mixtures. This linear dependence of the peak position on cholesterol concentration seems peculiar when one considers that the cholesterol molecule has a projected area of approximately 38 Å^2, whereas for DPPC, SM, and ceramide the projected area of each alkyl chain is roughly 20 Å^2.

It was suggested that the system has fixed cholesterol/lipid stoichiometries, and the smooth transition of the broad Bragg peak represents a superposition of distinct peaks.[10d,32] An alternative interpretation is that cholesterol forms ordered domains at all ratios and the area per molecule varies as a result of a position shift of the cholesterol along the perpendicular axis of the membrane.[9f] The coherence length of the mixed phase domains is approximately 2 nm, corresponding to roughly 10–15 molecules. Therefore, the broad peaks may also be interpreted to arise from a close-to-amorphous material with a typical average distance between molecules.

In bilayers, the behavior of the mixed phase is different. The position of the slope and plateau lines taken from the monolayer plot do not reflect the *d*-spacings in the bilayer, which in turn differ for SM/Chol, DPPC/Chol, and Cer/Chol mixtures with the same ratios. Furthermore, in bilayers each of the mixtures has a typical cholesterol concentration from which cholesterol nucleates to form pure cholesterol bilayer crystals (Figure 6, marked by colored bands). Beyond the threshold composition two phases co-exist in the bilayer owing to interactions at the membrane's core between the opposing leaflets, whereas in the monolayer there is only one mixed phase. Analogously, in DPPC/Chol bilayers a pure DPPC phase and a mixed DPPC/Chol phase were observed to coexist for the 60:40 mol ratio, whereas in the monolayer only one mixed phase is observed (Figure 7).[9g] The significance of cholesterol nucleation is discussed further in Section 4.2.

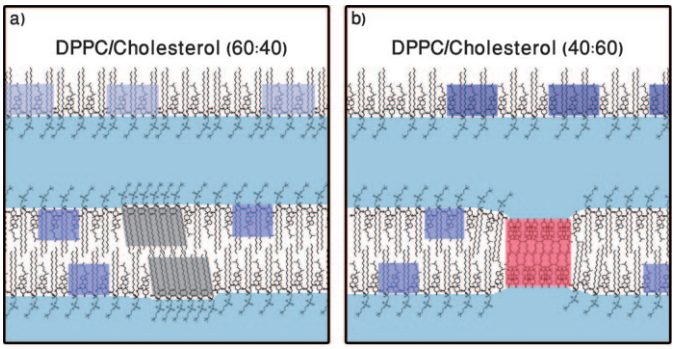

Figure 7. Schematic representation of a) a monolayer (top) and a bilayer (bottom) of DPPC/Chol (60:40) and b) a monolayer (top) and a bilayer (bottom) of DPPC/Chol (40:60). The phase behavior at both compositions in the bilayer differs from that of the corresponding monolayers. One crystalline mixed phase exists in each monolayer, colored in light blue for DPPC/Chol (60:40) and dark blue for DPPC/Chol (40:60), whereas phase separation occurs in the respective bilayers. Both bilayers have a similar mixed phase composition which is estimated to be DPPC/Chol (approximately 50:50). The additional phases are in (a) crystalline DPPC (gray) and in (b) crystalline cholesterol bilayers (red).

As an example where the unit cell of the crystalline domains depends strongly on the number of juxtaposed layers, we focus on ceramide C16/cholesterol mixtures. Figure 8 shows Bragg peaks of ceramide and Cer/Chol mixtures with 35–40 mol % ceramide from monolayers,[22] single bilayers,[53] and nonoriented multilayers, that is, multilamellar vesicles (MLVs).[11d] The pure ceramide C16 monolayer and bilayer yield one diffraction peak belonging to a previously studied unit cell.[11c] In the multilayer diffraction there are several peaks which are much sharper relative to the bilayer, indicative of a longer coherence length of approximately 45 nm. At 40 mol % ceramide the monolayer shows two broad bands, one probably corresponding to pure ceramide with a short coherence length, the other to a ceramide/cholesterol mixture. In the bilayer, the same phases are accompanied by sharp diffraction of two crystalline cholesterol polymorphs. In the multilayer, one broad peak, likely corresponding to ceramide, appears together with sharp diffraction of a

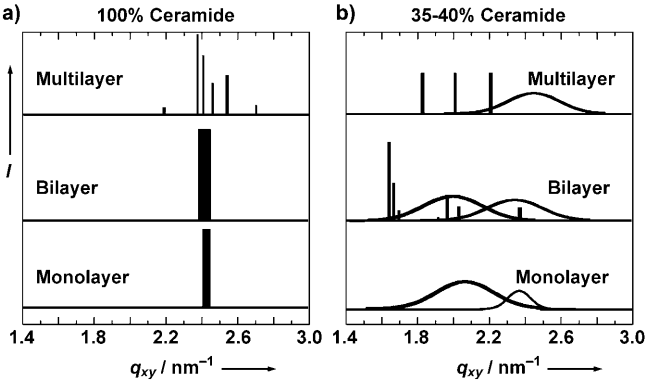

Figure 8. Schematic representation of Bragg peaks from GIXD of: bottom: Cer/Chol monoloayer mixtures deposited at the air–water interface and compressed to 30 mN m^{-1}; middle: Cer/Chol bilayer mixtures deposited at 30 mN m^{-1},[53] and top: from WAXS of Cer/Chol multilamellar vesicle mixtures.[11d] a) 100% ceramide C16; b) Mono- and bilayers are composed of Cer/Chol (40:60) and the multilayer sample is composed of Cer/Chol (35:65). GIXD measurements were performed at 7 °C and WAXS at ambient temperature.

unidentified crystalline phase. Clearly the crystalline structures observed for the bilayer and multilayers are different.

3. Lipid Domains Studied by X-Ray Diffraction and Other Techniques

3.1. Structure and Dynamics

X-ray diffraction provides structural knowledge at a sub-angstrom scale and is the only method that provides information on the periodicity of the crystalline domains. The duration of an X-ray diffraction measurement on thin films at interfaces ranges from minutes to hours; therefore these studies lack information on the dynamics of lipid domains, which are estimated to occur on much shorter time scales. NMR and FTIR measurements require substantially less time, but similar to diffraction studies they provide data averaged over large volumes. In contrast to X-ray diffraction, these techniques are sensitive to the entire lipid sample rather than selectively to the crystalline domains, which can be an advantage or a disadvantage depending on the conditions. NMR spectroscopy may provide information on the dynamics of the domains in terms of order and diffusion rates.[33] NMR spectroscopy is sensitive to molecular interactions, and is thus routinely used to decipher the macroscale structure of membranes, that is, to distinguish between vesicle, rodlike, and lamellar structures.[34] FTIR spectroscopy may be used to study the molecular orientation within the lipid sheets[35] and is very useful for monitoring structural transitions upon changes in the sample environment.

3.2. Localization

The footprint of the X-ray beam is tens of mm^2 for the grazing incidence techniques and <1 mm^2 for measurements of MLVs, and the diffraction signal arises from all irradiated crystalline domains. Therefore, the methods described above cannot provide information regarding the domain position in space or their distribution. It is thus unclear whether the domains are distributed evenly in the sample or clustered together forming a mosaiclike arrangement. During GIXD measurements the sample is not rotated, such that only a small part of the crystalline domains contribute to the diffraction signal, depending on their orientation, because the domains are randomly oriented as in a two-dimensional powder. Other methodologies, such as fluorescence microscopy[36] and electron microscopy (EM) appear better suited for studies of lipid domain localization at the micrometer and nanometer scale, respectively. Only few cryo-EM studies have been published to date, which directly localize lipid domains, rather than labeling the proteins associated with them. This technique is potentially the most promising in terms of resolution and accuracy.[37]

3.3. Lipid Phases

Lipid phase behavior has been extensively studied in relation to the formation of lipid domains in cell membranes, and the information obtained from X-ray diffraction must be related to this wealth of existing information. Lipid phases have been studied by several techniques, including NMR,[33] FTIR,[35] and fluorescence spectroscopy,[36b,38] and calorimetry. Unfortunately, the obtained phase diagrams differ for each method.[39] Nevertheless, there is sufficient agreement between the results obtained with the different methods to allow some consensus on the general behavior of phases.

The phases co-existing in lipid mixtures are sorted by their melting temperature into liquid disordered (l_d), liquid ordered (l_o), and solid ordered (S_o, also referred to as "gel-like domains"), and each is characterized by a different diffusion coefficient.

In most cases there seems to be a correlation between the crystalline domains and phase behavior for the studied cases of saturated lipid mixtures. To distinguish between the concept of domain as defined by phase separation and diffraction, we shall refer to these as "phase domains" and "crystalline domains", respectively. In particular, it is noteworthy that at compositions where the mixtures are reported to be in the l_o phase the coherence lengths of the crystalline domains are found to be a few nanometers. In contrast, at compositions where the S_o phase is reported to exist, the coherence lengths of the crystalline domains are measured to be tens of nanometers (Figures 9 and 10).

There is, however, also disagreement between phase diagrams and crystalline behavior: unlike what may be concluded from ternary/binary phase diagrams, at high levels cholesterol forms a S_o phase and most certainly does not remain as a liquid (l_o or l_d) phase (Figure 10). In addition, these phase diagrams all define pure SM as a solid ordered phase, whereas GIXD studies show that the opposite is true: in terms of coherence lengths SM appears to be in a l_o phase only when compressed. It will be interesting to readdress the issue of phase domains versus crystalline domains once more

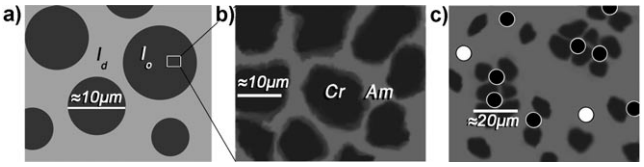

Figure 9. a) Schematic representation of the phase separation that would be detected with an optical microscope in phase domains. Light gray represents a l_d phase, whereas dark gray represents a l_o phase composed mostly of saturated lipids. b) According to our interpretation, a closer look at the l_o phase would reveal crystalline domains (*Cr*) surrounded by an amorphous phase (*Am*). c) Proteins, represented by black and white circles, may aggregate with the crystalline lipid domains leading to larger domains.[28b] The process may be selective for black proteins, whereas white proteins remain unbound.

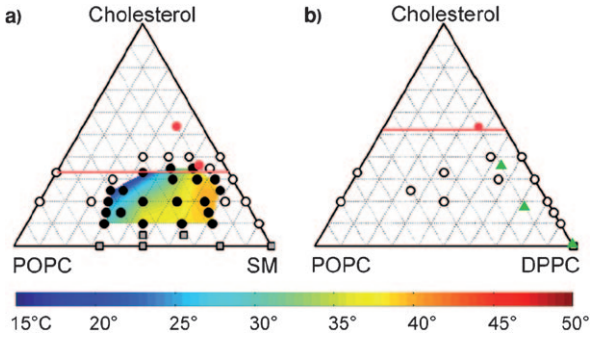

Figure 10. Miscibility phase boundaries in ternary lipid mixtures of a) POPC/SM/Chol and b) POPC/DPPC/Chol). Compositions where a miscibility transition is observed are denoted by filled black circles and the colored surface reports an extrapolated fit of the measured transition temperatures. Open circles indicate that only one liquid phase is present down to 10 °C. Gray squares indicate that solid domains nucleate directly from a uniform liquid phase as the temperature is lowered.[36a] Red circles represent compositions at which cholesterol bilayer crystals were measured by GIXD on bilayers, and red lines show an estimated cholesterol nucleation threshold. Green triangles represent crystalline DPPC domains. Mixed crystalline domains (not marked) are also observed for both SM/Chol and DPPC/Chol systems at most ratios. The colored symbols represent measurements on supported bilayers at 7 °C, whereas the original data is obtained from vesicles at 15–50 °C. The threshold red line may shift to higher cholesterol levels as the temperature is raised; nevertheless, cholesterol crystals were also observed at 37 °C. Reproduced with permission from Ref. [36a], with addition of the red dots, lines, and green triangles; PSM (palmitoyl SM) was changed to SM.

complete information is available in both areas.[15c,40] The position of the new line for the $l_o + S_o$ phase boundary may even occur at cholesterol concentrations relevant to vesicle studies.[19]

Phase domains are observed to grow in vitro up to the micrometer scale, whereas in cell membranes the functional domains are believed to be on the order of tens of nanometers, within the range of those measured by X-ray diffraction. We note that the micrometer-scale regions measured in phase domains may well be composed of a mosaic arrangement of the nanodomains measured by GIXD, possibly delimited by amorphous boundaries where unsaturated lipids may reside (Figure 9). Such an interpretation may provide an explanation for the discrepancies in domain size between artificial membranes and cell membranes, which is still the subject of lively discussions.[28b,30,31,41] Whereas the size of the fundamental structural unit of all domains would remain in the same range of tens of nanometers, phase domains grow to the micrometer scale as equilibrium is approached, a situation never achieved in cells.

4. Crystalline Lipid Domains Studied by X-Ray Diffraction in Relation to Biology

4.1. Protein Sorting

The protein-sorting mechanism among different lipid domains is not well understood. Three different hypotheses have been formulated: 1) Membrane thickness may control the incorporation of proteins according to the thickness of their hydrophobic moiety. 2) Similarly, the hydrophobic moiety also determines the local membrane curvature, which may contribute to the selection of proteins having a congenial geometry.[42] 3) The separation of the lipid phase into ordered and disordered domains is exploited.

Some tens of lipids would, however, probably be sufficient in order to achieve protein sorting through the three protein sorting mechanisms discussed above, which does not explain why cells have thousands of different lipids. In addition, membrane thickness and curvature, and the few compositional domains formed by phase separation are unlikely to achieve the selective sorting of thousands of membrane proteins. The wealth of structures found to exist in the nanometer-size crystalline lipid domains can contribute an additional hierarchical level to the sorting of proteins, according to their structural and chemical complementarities. The unit cell dimensions and the ordered periodicity may well reflect alkyl chain distances potentially affecting the interactions with nonlipid membrane molecules, such as proteins.

Hancock[28b] has suggested that the interactions between proteins and lipid nanodomains lead to the formation of larger and more stable clusters of domains with a prolonged lifetime (Figure 9). The crystalline domains discussed here may serve as building blocks of these clusters.

4.2. Cholesterol Nucleation

Cholesterol levels in the plasma membrane have been reported to be as high as 25–50 %.[8,43] Considering that the lipids are not spread homogenously in the membrane, the local concentration of cholesterol can reach very high levels. Therefore the thresholds for cholesterol nucleation observed in artificial bilayer mixtures are relevant to the actual levels in cells. Formation of the cholesterol crystals studied by X-ray diffraction suggests that the 3D cholesterol crystals, which lead to atherosclerosis inflammation and formation of atherosclerotic plaques,[44] may nucleate from the cytoplasmic membranes.[45] It is interesting to speculate how the local composition of the cell membrane may control the segregation of cholesterol into specific domains, and, upon failure of

the control mechanism, may result in nucleation of cholesterol crystals, triggering a chain reaction eventually leading to disease.

4.3. Which Technique To Use?

Technically, each diffraction method for studying lipid layer organization has its advantages and disadvantages, as detailed above. When applied to biologically relevant systems, the method to be selected is more straightforward: The multilayer method (Figure 4) is likely to be more relevant for nucleation studies of 3D lipid crystals, and multilamellar systems such as the stratum corneum[11d,46] and the pulmonary surfactant.[47] The pulmonary surfactant has relatively few layers of lipids exposed to air on one side. Therefore, GIXD performed on a Langmuir trough (Figure 1) is also relevant for these studies and has the advantage of dynamic compression control of the lipid sheets, imitating the compression and decompression states that occur during air flow in and out of the lungs.

The bilayer methods (Figure 2) are more relevant for studying cell membranes; however, so far they have been used only to study symmetrical bilayers. Although it is known that in cells the lipids are asymmetrically distributed between the membrane leaflets,[48] the specific composition in each leaflet is uncertain, and the actual composition in the nanoscale of the lipid domains in opposing leaflets is completely unknown. Apart from the cholesterol bilayer, no structural coupling of leaflets has been observed in the symmetric bilayer samples that have been examined to date. To what extent the bilayer method can be advantageous in establishing interactions between opposing leaflets is thus unclear, until the actual compositions have been determined.

5. Concluding Remarks

Cell membrane bilayers are composed of thousands of lipid molecules with different chemical compositions and molecular structures. X-ray diffraction methods have become available recently, which allow the determination of structural parameters of periodical structures in thin layers of lipids. Application of these techniques reveals the existence of a variety of crystalline domain structures in model monolayer, bilayer, and multilayer lipid mixtures. These are ordered arrays of molecules, typically few tens of nm in diameter and in dynamic exchange with the environment, primarily stabilized by intermolecular interactions along the extended aliphatic chains.

We suggest that this variety of structures reflects an additional hierarchical level of organization that may be essential in the understanding of cell membrane function. The existence of such crystalline domains may play an important role in protein sorting, phase separation, and pathological crystallizations, and may reconcile the discrepancies between the domain sizes and structures observed in artificial systems, relative to those found in biological membranes.

We thank HASYLAB for synchrotron beamtime and ELISA: EU financial support of access to synchrotrons/FELs in Europe. This work was supported by the Israel Science Foundation and the Helen and Martin Kimmel Center for Nanoscale Science. L.A. is the incumbent of the Dorothy and Patrick Gorman Professorial Chair of Biological Ultrastructure.

Received: July 21, 2010
Published online: February 25, 2011

[1] B. Alberts, *Molecular Biology of the Cell*, *4th ed.*, Garland Science, New York, **2002**.
[2] a) D. A. Brown, J. K. Rose, *Cell* **1992**, *68*, 533–544; b) D. A. Brown, E. London, *Biochem. Biophys. Res. Commun.* **1997**, *240*, 1–7; c) K. Simons, D. Toomre, *Nat. Rev. Mol. Cell Biol.* **2000**, *1*, 31–39; d) K. Simons, E. Ikonen, *Nature* **1997**, *387*, 569–572; e) M. F. Hanzal-Bayer, J. F. Hancock, *FEBS Lett.* **2007**, *581*, 2098–2104.
[3] a) E. Ikonen, *Physiol. Rev.* **2006**, *86*, 1237–1261; b) F. R. Maxfield, I. Tabas, *Nature* **2005**, *438*, 612–621.
[4] R. P. Mason, T. N. Tulenko, R. F. Jacob, *Biochim. Biophys. Acta Biomembr.* **2003**, *1610*, 198–207.
[5] R. J. Cenedella, *JAMA J. Am. Med. Assoc.* **1987**, *257*, 1602–1602.
[6] D. Weihs, J. Schmidt, I. Goldiner, D. Danino, M. Rubin, Y. Talmon, F. M. Konikoff, *J. Lipid Res.* **2005**, *46*, 942–948.
[7] T. N. Tulenko, M. Chen, P. E. Mason, R. P. Mason, *J. Lipid Res.* **1998**, *39*, 947–956.
[8] G. van Meer, D. R. Voelker, G. W. Feigenson, *Nat. Rev. Mol. Cell Biol.* **2008**, *9*, 112–124.
[9] a) T. T. Mills, S. Tristram-Nagle, F. A. Heberle, N. F. Morales, J. Zhao, J. Wu, G. E. S. Toombes, J. F. Nagle, G. W. Feigenson, *Biophys. J.* **2008**, *95*, 682–690; b) T. T. Mills, J. Y. Huang, G. W. Feigenson, J. F. Nagle, *Gen. Physiol. Biophys.* **2009**, *28*, 126–139; c) A. Aroti, E. Leontidis, E. Maltseva, G. Brezesinski, *J. Phys. Chem. B* **2004**, *108*, 15238–15245; d) G. Brezesinski, A. Dietrich, B. Struth, C. Bohm, W. G. Bouwman, K. Kjaer, H. Mohwald, *Chem. Phys. Lipids* **1995**, *76*, 145–157; e) E. B. Watkins, C. E. Miller, D. J. Mulder, T. L. Kuhl, J. Majewski, *Phys. Rev. Lett.* **2009**, *102*, 238101; f) A. Ivankin, I. Kuzmenko, D. Gidalevitz, *Phys. Rev. Lett.* **2010**, *104*, 108101; g) R. Ziblat, L. Leiserowitz, L. Addadi, *J. Am. Chem. Soc.* **2010**, *132*, 9920–9927.
[10] a) D. Vaknin, M. S. Kelley, B. M. Ocko, *J. Chem. Phys.* **2001**, *115*, 7697–7704; b) C. Chachaty, D. Rainteau, C. Tessier, P. J. Quinn, C. Wolf, *Biophys. J.* **2005**, *88*, 4032–4044; c) G. Staneva, C. Chachaty, C. Wolf, P. J. Quinn, *J. Lipid Res.* **2010**, *51*, 1810–1822; d) M. K. Ratajczak, E. Y. Chi, S. L. Frey, K. D. Cao, L. M. Luther, K. Y. C. Lee, J. Majewski, K. Kjaer, *Phys. Rev. Lett.* **2009**, *103*, 28103; e) C. Ege, M. K. Ratajczak, J. Majewski, K. Kjaer, K. Y. C. Lee, *Biophys. J.* **2006**, *91*, L1L3.
[11] a) G. Staneva, C. Chachaty, C. Wolf, K. Koumanov, P. J. Quinn, *Biochim. Biophys. Acta Biomembr.* **2008**, *1778*, 2727–2739; b) L. Scheffer, A. H. Futerman, L. Addadi, *ChemBioChem* **2007**, *8*, 2286–2294; c) D. Vaknin, M. S. Kelley, *Biophys. J.* **2000**, *79*, 2616–2623; d) S. L. Souza, M. J. Capitan, J. Alvarez, S. S. Funari, M. H. Lameiro, E. Melo, *J. Phys. Chem. B* **2009**, *113*, 1367–1375.
[12] a) R. J. Schroeder, S. N. Ahmed, Y. Z. Zhu, E. London, D. A. Brown, *J. Biol. Chem.* **1998**, *273*, 1150–1157; b) K. Fiedler, T. Kobayashi, T. V. Kurzchalia, K. Simons, *Biochemistry* **1993**, *32*, 6365–6373; c) C. Arnulphi, J. Sot, M. Garcia-Pacios, J. L. R. Arrondo, A. Alonso, F. M. Goni, *Biophys. J.* **2007**, *93*, 3504–3514.
[13] D. M. Small, *Handbook of Lipid Research: The Physical Chemistry of Lipids*, *Vol. 4*, Plenum Press, New York, **1986**.

[14] T. J. Mcintosh, *Biochim. Biophys. Acta Biomembr.* **1978**, *513*, 43 – 58.

[15] a) K. Kjaer, J. Als-Nielsen, C. A. Helm, L. A. Laxhuber, H. Mohwald, *Phys. Rev. Lett.* **1987**, *58*, 2224 – 2227; b) P. Dutta, J. B. Peng, B. Lin, J. B. Ketterson, M. Prakash, P. Georgopoulos, S. Ehrlich, *Phys. Rev. Lett.* **1987**, *58*, 2228 – 2231; c) V. M. Kaganer, H. Mohwald, P. Dutta, *Rev. Mod. Phys.* **1999**, *71*, 779 – 819.

[16] J. Als-Nielsen, D. Jacquemain, K. Kjaer, F. Leveiller, M. Lahav, L. Leiserowitz, *Phys. Rep.* **1994**, *246*, 252 – 313.

[17] E. Sackmann, H. Trauble, *J. Am. Chem. Soc.* **1972**, *94*, 4482-4491.

[18] a) C. E. Miller, J. Majewski, E. B. Watkins, D. J. Mulder, T. Gog, T. L. Kuhl, *Phys. Rev. Lett.* **2008**, *100*, 58103; b) I. Solomonov, J. Daillant, G. Fragneto, K. Kjaer, J. S. Micha, F. Rieutord, L. Leiserowitz, *Eur. Phys. J. E: Soft Matter Biol. Phys.* **2009**, *30*, 215 – 221; c) J. Daillant, *Curr. Opin. Colloid Interface Sci.* **2009**, *14*, 396 – 401.

[19] R. Ziblat, K. Kjaer, L. Leiserowitz, L. Addadi, *Angew. Chem.* **2009**, *121*, 9120 – 9123; *Angew. Chem. Int. Ed.* **2009**, *48*, 8958 – 8961.

[20] a) R. P. Rand, V. Luzzati, *Biophys. J.* **1968**, *8*, 125-137; b) L. A. Feigin, D. I. Svergun, *Structure Analysis by Small-Angle X-Ray and Neutron Scattering*, Plenum Press, New York, **1987**.

[21] I. Kuzmenko, H. Rapaport, K. Kjaer, J. Als-Nielsen, I. Weissbuch, M. Lahav, L. Leiserowitz, *Chem. Rev.* **2001**, *101*, 1659 – 1696.

[22] L. Scheffer, I. Solomonov, M. J. Weygand, K. Kjaer, L. Leiserowitz, L. Addadi, *Biophys. J.* **2005**, *88*, 3381 – 3391.

[23] M. K. Ratajczak, C. Ege, Y. T. C. Ko, J. Majewski, K. Kjaer, K. Y. C. Lee, *Biophys. J.* **2005**, *88*, 73a-73a.

[24] J. Y. Huang, G. W. Feigenson, *Biophys. J.* **1999**, *76*, 2142 – 2157.

[25] H. Rapaport, I. Kuzmenko, S. Lafont, K. Kjaer, P. B. Howes, J. Als-Nielsen, M. Lahav, L. Leiserowitz, *Biophys. J.* **2001**, *81*, 2729 – 2736.

[26] I. Solomonov, M. J. Weygand, K. Kjaer, H. Rapaport, L. Leiserowitz, *Biophys. J.* **2005**, *88*, 1809 – 1817.

[27] B. M. Craven, *Nature* **1976**, *260*, 727 – 729.

[28] a) K. Simons, W. L. C. Vaz, *Annu. Rev. Biophys. Biomol. Struct.* **2004**, *33*, 269 – 295; b) J. F. Hancock, *Nat. Rev. Mol. Cell Biol.* **2006**, *7*, 456 – 462.

[29] L. D. Landau, E. M. Lifshitz, *Statistical Physics*, *3rd. ed.*, *Vol. 5*, Pergamon, **1980**.

[30] R. Brewster, P. A. Pincus, S. A. Safran, *Biophys. J.* **2009**, *97*, 1087 – 1094.

[31] R. Brewster, S. A. Safran, *Biophys. J.* **2010**, *98*, L21 – L23.

[32] a) H. M. McConnell, A. Radhakrishnan, *Biochim. Biophys. Acta Biomembr.* **2003**, *1610*, 159 – 173; b) H. M. McConnell, M. Vrljic, *Annu. Rev. Biophys. Biomol. Struct.* **2003**, *32*, 469 – 492.

[33] C. P. S. Tilcock, P. R. Cullis, S. M. Gruner, *Chem. Phys. Lipids* **1986**, *40*, 47 – 56.

[34] A. M. Dopico, *Methods in Membrane Lipids*, *Vol. 400*, Humana, New York, **2007**.

[35] a) R. D. Hunt, M. L. Mitchell, R. A. Dluhy, *J. Mol. Struct.* **1989**, *214*, 93 – 109; b) G. Brezesinski, H. Möhwald, *Adv. Colloid Interface Sci.* **2003**, *100*, 563 – 584.

[36] a) S. L. Veatch, S. L. Keller, *Phys. Rev. Lett.* **2005**, *94*, 148101; b) S. N. Pinto, L. C. Silva, R. F. M. deAlmeida, M. Prieto, *Biophys. J.* **2008**, *95*, 2867 – 2879.

[37] a) F. M. Konikoff, D. Danino, D. Weihs, M. Rubin, Y. Talmon, *Hepatology* **2000**, *31*, 261 – 268; b) J. Majewski, L. Margulis, *Langmuir* **1994**, *10*, 2081 – 2083; c) V. Weissig, *Liposomes: Methods and Protocols*, *Vol. 2 (Biological Membrane Models)*, Humana, New York, **2010**; d) D. Weihs, J. Schmidt, D. Danino, I. Goldiner, D. Leikin-Gobbi, A. Eitan, M. Rubin, Y. Talmon, F. M. Konikoff, *Biochim. Biophys. Acta Mol. Cell Biol. Lipids* **2007**, *1771*, 1289 – 1298.

[38] a) S. L. Veatch, S. L. Keller, *Biophys. J.* **2003**, *85*, 3074 – 3083; b) B. M. Castro, L. C. Silva, A. Fedorov, R. F. M. deAlmeida, M. Prieto, *J. Biol. Chem.* **2009**, *284*, 22978 – 22987.

[39] F. M. Goni, A. Alonso, L. A. Bagatolli, R. E. Brown, D. Marsh, M. Prieto, J. L. Thewalt, *Biochim. Biophys. Acta Mol. Cell Biol. Lipids* **2008**, *1781*, 665 – 684.

[40] G. W. Feigenson, *Biochim. Biophys. Acta Biomembr.* **2009**, *1788*, 47 – 52.

[41] a) S. L. Veatch, O. Soubias, S. L. Keller, K. Gawrisch, *Proc. Natl. Acad. Sci. USA* **2007**, *104*, 17650 – 17655; b) A. R. Honerkamp-Smith, P. Cicuta, M. D. Collins, S. L. Veatch, M. den Nijs, M. Schick, S. L. Keller, *Biophys. J.* **2008**, *95*, 236 – 246; c) G. S. Longo, M. Schick, I. Szleifer, *Biophys. J.* **2009**, *96*, 3977 – 3986.

[42] a) O. S. Andersen, R. E. Koeppe, *Annu. Rev. Biophys. Biomol. Struct.* **2007**, *36*, 107 – 130; b) R. Phillips, T. Ursell, P. Wiggins, P. Sens, *Nature* **2009**, *459*, 379 – 385.

[43] E. Ikonen, *Nat. Rev. Mol. Cell Biol.* **2008**, *9*, 125 – 138.

[44] P. Duewell, H. Kono, K. J. Rayner, C. M. Sirois, G. Vladimer, F. G. Bauernfeind, G. S. Abela, L. Franchi, G. Nunez, M. Schnurr, T. Espevik, E. Lien, K. A. Fitzgerald, K. L. Rock, K. J. Moore, S. D. Wright, V. Hornung, E. Latz, *Nature* **2010**, *464*, 1357-1361.

[45] D. S. Ong, J. J. Anzinger, F. J. Leyva, N. Rubin, L. Addadi, H. S. Kruth, *J. Lipid Res.* **2010**, *51*, 2303 – 2313.

[46] a) J. A. Bouwstra, G. S. Gorris, K. Cheng, A. Weerheim, W. Bras, M. Ponec, *J. Lipid Res.* **1996**, *37*, 999 – 1011; b) T. J. McIntosh, M. E. Stewart, D. T. Downing, *Biochemistry* **1996**, *35*, 3649 – 3653.

[47] a) P. C. Stenger, G. H. Wu, C. E. Miller, E. Y. Chi, S. L. Frey, K. Y. C. Lee, J. Majewski, K. Kjaer, J. A. Zasadzinski, *Biophys. J.* **2009**, *97*, 777 – 786; b) K. Y. C. Lee, J. Majewski, T. L. Kuhl, P. B. Howes, K. Kjaer, M. M. Lipp, A. J. Waring, J. A. Zasadzinski, G. S. Smith, *Biophys. J.* **2001**, *81*, 572 – 585.

[48] M. Bretsche, *Nature New Biol.* **1972**, *236*, 11-12.

[49] a) R. Merkel, E. Sackmann, E. Evans, *J. Phys. (Paris)* **1989**, *50*, 1535 – 1555; b) E. Evans, E. Sackmann, *J. Fluid Mech.* **1988**, *194*, 553 – 561.

[50] E. Sackmann, *Science* **1996**, *271*, 43 – 48.

[51] W. J. Sun, R. M. Suter, M. A. Knewtson, C. R. Worthington, S. Tristramnagle, R. Zhang, J. F. Nagle, *Phys. Rev. E* **1994**, *49*, 4665 – 4676.

[52] T. T. Mills, G. E. S. Toombes, S. Tristram-Nagle, D. M. Smilgies, G. W. Feigenson, J. F. Nagle, *Biophys. J.* **2008**, *95*, 669 – 681.

[53] R. Ziblat, PhD Thesis, Weizmann Institute of Science.

